The radial velocity and metal abundance of the Sextans dwarf spheroidal galaxy

G. S. Da Costa and D. Hatzidimitriou
Anglo–Australian Observatory, PO Box 296, Epping, NSW 2121, Australia

M. J. Irwin and R. G. McMahon
Institute of Astronomy, Madingley Road, Cambridge CB3 0HA

SUMMARY

The AAT FOCAP fibre system has been used to obtain spectra, centred at the Ca II IR-triplet, of 14 stars in the field of the recently discovered Sextans dwarf spheroidal galaxy. Radial velocities derived from these spectra indicate that six of the stars observed are Sextans members. Their velocities cluster closely about a value of 230 ± 6 km s^{-1} which we take as the heliocentric velocity of this galaxy. This velocity, when corrected to the galactic rest frame, indicates that Sextans makes a contribution comparable to those of other dSph galaxies, such as Sculptor and Ursa Minor, to calculations of the mass of the galaxy's halo. The spectra of the Sextans members also yield an estimate of the mean abundance of this galaxy: a value of [Fe/H] $= -1.7 \pm 0.25$ dex is suggested from a comparison of the line strengths with those of globular cluster stars. This value is higher than that expected for Sextans from the absolute magnitude–abundance relation, followed by the other galactic dSph galaxies.

1 INTRODUCTION

The recent discovery (Irwin *et al.* 1990) of a new dwarf spheroidal (dSph) galaxy in the constellation of Sextans raised to eight the number of known companions to the Milky Way of this type. While the basic properties of the Sextans system were established in the discovery paper, a number of important quantities remain to be determined. These include the mean abundance, the presence or absence of any abundance spread, the age of the population and the extent of any age range, and the galaxy's mean velocity, velocity dispersion and mass-to-light ratio. These latter quantities are of considerable interest since the dSph galaxies of similar luminosity to Sextans, namely Draco and Ursa Minor, show clear evidence for the presence of substantial amounts of dark matter (e.g. Pryor & Kormendy 1990), while the more luminous systems generally do not (e.g. Da Costa 1988).

The determination of some of these quantities depends on the isolation of a sample of Sextans members. This is most easily done if the systemic velocity of the galaxy is known, provided of course that the velocity is substantially different from that of foreground field stars. The purpose of this paper then, is to describe the determination of the systemic velocity of the Sextans system from observations of a sample of stars in a Sextans field. This velocity is also important for another reason. The radial velocities and distances of the stellar systems (i.e. both globular clusters and dSph galaxies) in the outer halo are frequently used to constrain the mass of the galaxy. A determination of the radial velocity of Sextans will add weight to these estimates by increasing the size of the small sample of objects on which they are based.

The observations and reductions are described in the next section, while Section 3 details the systemic velocity determination. Also discussed in this section is the derivation of a first estimate of the mean metal abundance for this dSph galaxy. The implications of the Sextans radial velocity for the mass of the galaxy and the consequences of the mean metal abundance estimate are discussed in the final section.

2 OBSERVATIONS AND REDUCTIONS

Using the $c-m$ diagram of Irwin *et al.* (1990) as a guide, a sample of approximately 60 candidate Sextans giants was selected for observation with the AAT FOCAP fibre system. This system allows coverage of a 40-arcmin diameter field with the fibres being held in place by a precisely drilled brass plate. The required accurate coordinates for the candidate giants, as well as for a few bright fiducial (guide) stars, were automatically available from the APM scans. A 320-μm (2 arcsec in the focal plane) fibre bundle was employed which feeds into the RGO Spectrograph. A 600-line grating,

mounted blaze-to-camera and centred at $\lambda 8550$A, was used in the spectrograph with a front-illuminated Thomson CCD serving as detector in the 25-cm camera. This CCD, which has 19 μm pixels and a readout noise of only 3e⁻, is cosmetically almost perfect with a very uniform response and extremely good charge transfer. This latter property is especially important given the large number of bright emission lines in the sky spectrum that must be accurately subtracted to reveal the object spectra. A 1024×512 CCD window was employed with no on-chip binning, giving a wavelength coverage of over 1000 Å at 1.21 Å pixel⁻¹ or 42.4 km s⁻¹ pixel⁻¹. The resolution was 3.2 Å (FWHM). Five of the 57 usable fibres in the bundle were allocated to blank sky regions.

The observations took place on the night of 1990 May 6 in a 2-hr interval drawn from Director's time. Conditions were far from ideal with a bright almost-full moon and varying amounts of thick cirrus cloud. Two 30-min integrations were obtained interspersed with a 500-s sky offset exposure to calibrate the relative sensitivities of the fibres. Short exposures were also obtained of three bright radial-velocity standards. A spectrum of a giant in the globular cluster NGC 4590 was also obtained with the identical set-up on the preceding night when conditions were even worse.

The two data frames were first combined and then the individual spectra were extracted and wavelength calibrated using the routines available in the FIGARO package. The sky fibres were co-added to improve the signal-to-noise of the sky spectrum which was then subtracted from the object spectra after scaling by the relative fibre transmissions. Despite the strength of the night-sky emission features, the sky subtraction process produced acceptable results. However, although nominally ~ 50 stars were observed, only 14 had sufficient signal-to-noise ratio at the completion of the reduction process to justify further analysis. These stars, together with their coordinates and photometry from the APM scans are listed in Table 1.

Table 1. Observational data.

APM No.	RA (1950)	Dec (1950)	R_{mag}	(B_J-R)	v_r (kms⁻¹)	Error (kms⁻¹)
(a) Sextans Members						
4	10 9 52.11	-1 07 35.5	16.2	1.7	224	11
5	10 10 8.94	-1 30 36.3	16.3	1.6	225	14
10	10 9 47.57	-1 36 58.0	16.4	1.8	226	15
11	10 10 34.64	-1 21 7.4	16.4	1.3	244	9
13	10 10 8.59	-1 18 0.7	16.5	1.6	241	15
15	10 11 17.91	-1 30 18.7	16.5	1.5	221	22
(b) Non-Members						
2	10 10 41.33	-1 24 7.9	16.1	1.4	85	28
3	10 10 10.84	-1 13 41.5	16.1	1.5	5	7
6	10 10 45.29	-1 09 52.7	16.3	1.6	22	15
12	10 11 33.42	-1 19 56.1	16.4	1.6	7	26
16	10 10 21.75	-1 36 46.6	16.6	1.6	14	7
17	10 10 38.64	-1 28 9.3	16.6	1.2	278	14
20	10 10 37.62	-1 19 29.2	16.7	1.4	96	25
29	10 10 10.32	-1 17 14.0	16.9	1.6	74	28

3 RESULTS

3.1 Radial velocities

To determine relative radial velocities, the spectra of the stars in the Sextans field were cross-correlated with the high-signal-to-noise spectra of the three radial-velocity standards, following the basic procedures outlined in Armandroff & Da Costa (1986). In particular, although the available wavelength coverage was more extensive, the cross-correlation window was restricted to the region $8415 < \lambda < 8715$ Å. This region includes the Ca II IR triplet, but it is relatively free of telluric absorption features and excludes the strongest night-sky emission lines which did not always subtract off perfectly.

Application of a heliocentric correction and addition of the standard star velocity then results in three (one for each standard star) determinations of the heliocentric velocity of each programme star. Given the low signal-to-noise ratio of these spectra, it is not surprising that these velocities have individual uncertainties of the order of 20 km s⁻¹. No systematic dependence on the standard star spectrum used was found and the differences between the individual determinations were consistent with the cross-correlation errors. Consequently, the three determinations were averaged. These velocities are also given in Table 1 along with the velocity uncertainty from the cross-correlation errors.

The zero-point of the velocity system was investigated in two ways. First, the spectra of the radial-velocity standards were cross-correlated with each other. In each case the standard velocities of the stars were successfully recovered with an average difference between the observed and standard values of less than 2 km s⁻¹. Secondly, the spectrum of the NGC 4590 giant I-10 (Harris 1975) was processed in the same way as the Sextans field stars. The velocity determined was -95 ± 3 km s⁻¹. Hesser, Shawl & Meyer (1986) list a velocity of -88 ± 8 km s⁻¹ for NGC 4590 based on three low-dispersion integrated spectra, while Zinn & West (1984) give -64 ± 20 km s⁻¹ from a single low-dispersion integrated spectrum, after correcting the tabulated velocity by -5 km s⁻¹ (see the discussion in Hesser *et al.* 1986). The agreement with the Hesser *et al.* velocity is entirely satisfactory and indicates no major zero-point uncertainty in our velocities; the Zinn & West velocity for NGC 4590 appears to be in error though the difference is only 1.5σ. We conclude, therefore, that the uncertainty in the zero-point of the velocities listed in Table 1 is less than 5 km s⁻¹.

A histogram of the observed radial velocities is shown in Fig. 1. Inspection of this figure and the data of Table 1 reveals a clustering of six stars whose velocities show a total range of only 23 km s⁻¹. We identify these stars as members of the Sextans system and adopt their mean velocity, 230 ± 6 km s⁻¹, as the systemic heliocentric velocity of the Sextans dwarf spheroidal galaxy. The uncertainty given represents the combination of the standard deviation of the mean velocity (± 4 km s⁻¹) and the estimated zero-point uncertainty of less than 5 km s⁻¹. The six Sextans members are identified in Fig. 2.

The star with the highest velocity in Fig. 1, APM 17, may also be a Sextans member. However, since its velocity differs from the mean of the other six stars identified as members by more than 3σ, we have chosen not to include this star in the calculation of the Sextans mean velocity. A more accurate velocity for APM 17 is needed before the possible Sextans
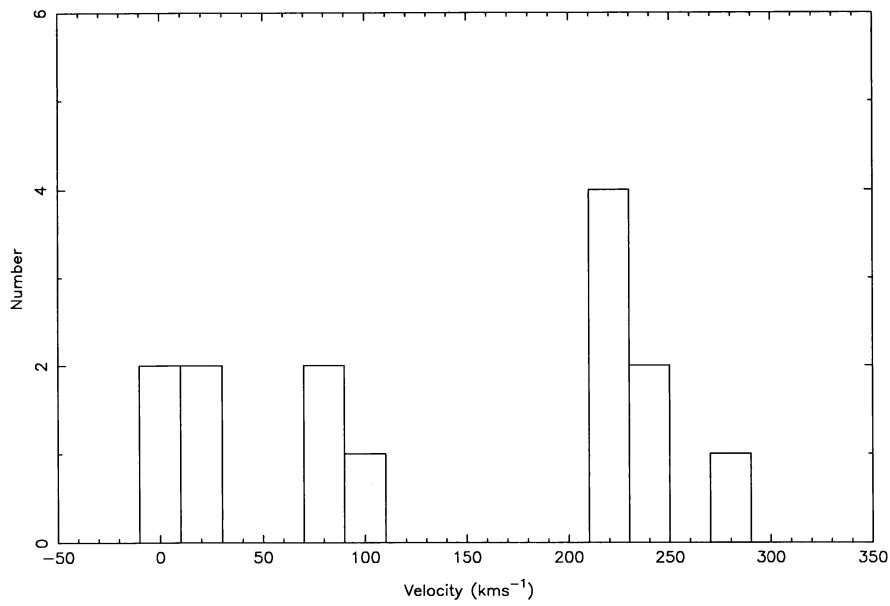
Figure 1. A histogram of velocities for the 14 stars observed in the field of the Sextans dwarf spheroidal galaxy. The bin width is 20 km s^{-1} which is comparable to the errors in the individual velocities. The stars in the prominent grouping at 230 km s^{-1} are taken as Sextans members.
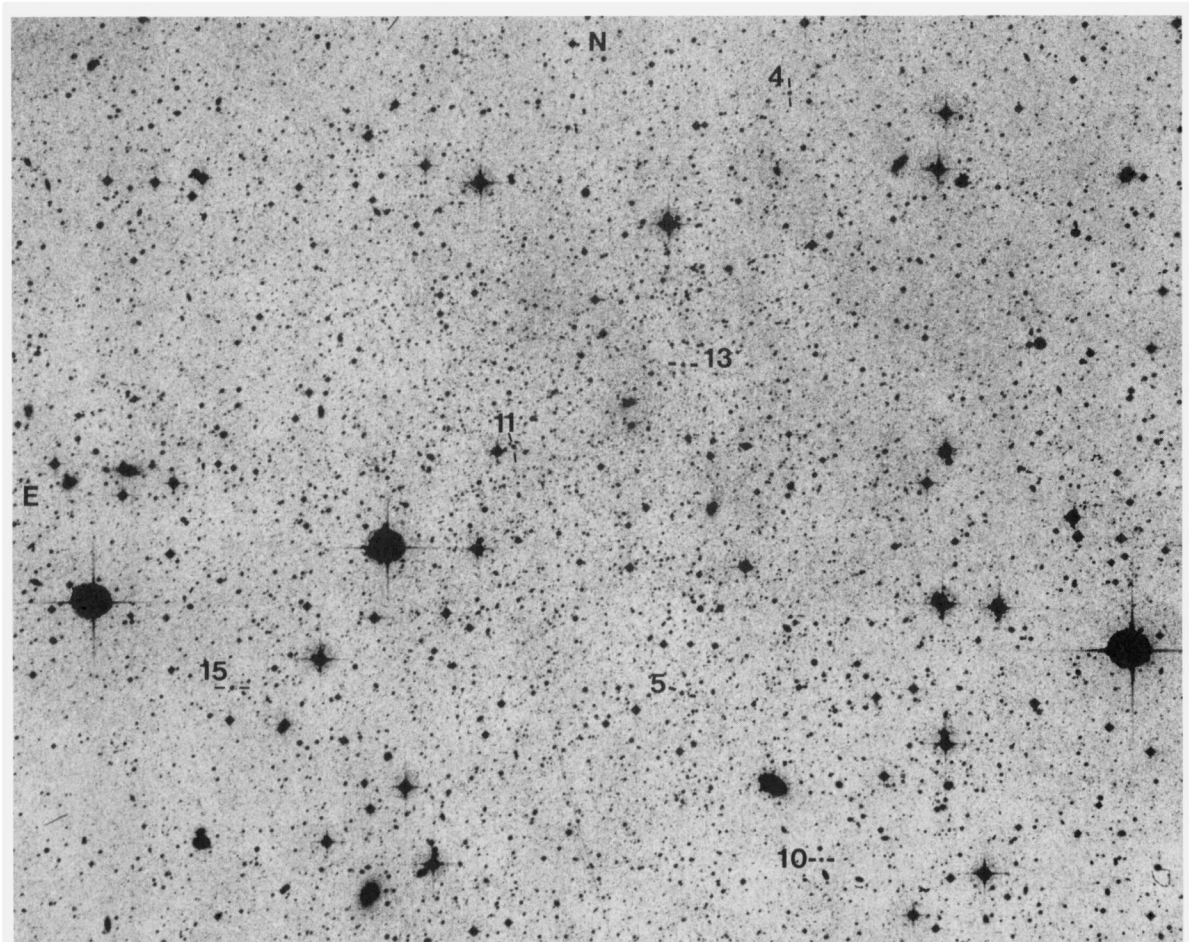
Figure 2. An identification chart for the six Sextans members. The numbers are those of Table 1. The print is made from a photographic composite of three SRC J Schmidt plates kindly provided by David Malin.

membership of this star can be definitely decided. As regards the other stars in Fig. 1, we identify them as follows, based on the Gilmore & Reid (1983) galaxy model: the stars with velocities near 30 km s^{-1} are local disc K and M dwarfs while those with velocities near 100 km s^{-1} are presumably thick-disc dwarfs.

One immediate consequence of our determination of the Sextans radial velocity is that it precludes any association between this dwarf galaxy and the sparse halo globular cluster Pal 3, which lies some 10 kpc or so beyond Sextans in the same part of the sky (Irwin *et al.* 1990). With a radial velocity of 89 ± 9 km s^{-1} (Olszewski, Peterson & Aaronson 1986), or some 141 ± 11 km s^{-1} less than that of Sextans, the current proximity of Pal 3 to Sextans must be ascribed to chance. We note also in passing that the observed velocity dispersion of the six Sextans members is only 9 km s^{-1} while the mean velocity error from the cross-correlation process is 14 km s^{-1}. Given the small sample size, however, this difference is not unexpected; there is a ~ 25 per cent probability that it arises by chance. There is thus no indication of the intrinsic velocity dispersion of Sextans in these data. However, an intrinsic dispersion of the order of 10 km s^{-1}, as is seen in the similar systems Draco and Ursa Minor (Aaronson & Olszewski 1988), can be ruled out only at the ~ 10 per cent significance level. Measurement of the intrinsic dispersion of the Sextans system, and its mass-to-light ratio, must await both an increased sample of members and more accurate velocities than those presented here. Nevertheless, the high value of the Sextans radial velocity will facilitate the identification of additional members.

3.2 Sextans metal abundance

Although the signal-to-noise ratio in any one of the six Sextans member spectra is low, the sum of these spectra can be used to make a first estimate of the mean metal abundance of this dwarf galaxy. This summed spectrum is shown in Fig. 3 along with the spectrum of the star in the metal-poor globular cluster NGC 4590, for which Zinn (1985) lists [Fe/H] = −2.09 dex.

To make such an abundance estimate, the equivalent widths of the Ca II lines at $\lambda 8550$ and $\lambda 8662$ were first measured using the techniques detailed in Armandroff & Da Costa (1991). Briefly, this involves fitting a continuum to the counts in bandpasses near the lines and then fitting a Gaussian to the resulting residual intensity. The sum of the two equivalent widths obtained from these spectra are 4.86 ± 0.72 for the summed Sextans spectra and 3.27 ± 0.14 for the NGC 4590 giant. Here the error listed is that associated with the uncertainty in the Gaussian fit which dominates any error due to uncertainty in the continuum location. These equivalent width measures are plotted against the absolute visual magnitude of the stars in Fig. 4. The value of M_V for NGC 4590 I-10 is based on the photometry of Harris (1975) for this star together with the assumption of $M_V = +0.6$ for the cluster horizontal branch. For Sextans, the point has been plotted at the absolute visual magnitude expected for stars near the giant branch tip, since no visual photometry is presently available for the stars observed. The photographic B and R magnitudes for these stars, however, are consistent with this assumption.

Fig. 4 also shows loci of constant abundance derived from similar observations of globular cluster giants. These latter observations, as described in Armandroff & Da Costa (1991), were obtained at Cerro Tololo Inter-American Observatory but, by a fortunate coincidence, they have closely similar resolution to the AAT observations. For this reason we do not expect any systematic uncertainties from the use of these abundance calibration lines, but the NGC 4590 I-10 observations provide a check. The location of this star in Fig. 4 yields an abundance of [Fe/H] = −2.07 ± 0.06 dex in excellent agreement with the abundance for this cluster, −2.09 ± 0.11 dex tabulated by Zinn & West (1984). Then, with this calibration, the equivalent widths determined from the summed Sextans spectra yield an abundance of [Fe/H] = −1.7 ± 0.25 dex which we take as a first estimate of the mean abundance of this dwarf galaxy. The error given reflects both the uncertainty in the equivalent widths and in the mean absolute visual magnitude of the stars. However, given the rather gentle slope of the calibration lines, this latter uncertainty is not the major one.

4   DISCUSSION

Assuming a solar motion of 16.5 km s^{-1} towards $(l, b) = (53, 25)$ (Delhaye 1965) and a circular velocity about the centre of the galaxy for the LSR of 220 km s^{-1}, the heliocentric velocity for Sextans derived above yields a galactic rest frame velocity of 78 km s^{-1} for this dSph galaxy. This value is comparable to that of other dSph galaxies (e.g. table 3 of Zaritsky *et al.* 1989) and combined with the large galactocentric distance of Sextans (~ 85 kpc, Irwin *et al.* 1990) indicates that Sextans deserves inclusion in discussions of the mass of the galaxy.

This point is illustrated in Fig. 5 which is an updated version of a diagram first introduced by Lynden-Bell, Cannon & Godwin (1983). This diagram plots three times the square of the galactic rest frame line-of-sight velocity for halo objects against galactocentric distance. In their analysis of the data available at that time, Lynden-Bell *et al.* (1983) noted that many of the outer halo objects had poorly determined velocities and/or distances and that this led to large 'observational' uncertainties in the galactic mass determinations. This is not the case now; the uncertainties in the parameters for the outer halo objects in Fig. 5 are much smaller than the spread exhibited in both coordinates.

With the exception of NGC 5824 for which the more recent V_{HB} determination of Cannon, Sagar & Hawkins (1990) was employed, the globular cluster points in Fig. 5 were deduced from the convenient compilation of reddenings, horizontal branch magnitudes and galactic rest frame velocities (v_r) for the halo, as distinct from the disc, globular clusters given by Armandroff (1989). Galactocentric distances were calculated assuming $M_V = +0.6$ for the horizontal branch, independent of metallicity, and a Sun−Galactic Centre distance of 8.5 kpc. The data for the outer halo objects were taken from Zaritsky *et al.* (1989) with the addition of Sextans as derived here. The individual halo globular cluster values were combined into bins of galactocentric distance with the mean values of $3v_r^2$ for the clusters with $R(\text{kpc}) < 5$, $5 < R < 10$, $10 < R < 20$ and $20 < R < 40$ shown as filled squares in the figure. The individual cluster points are also shown for the $20 < R < 40$ bin.
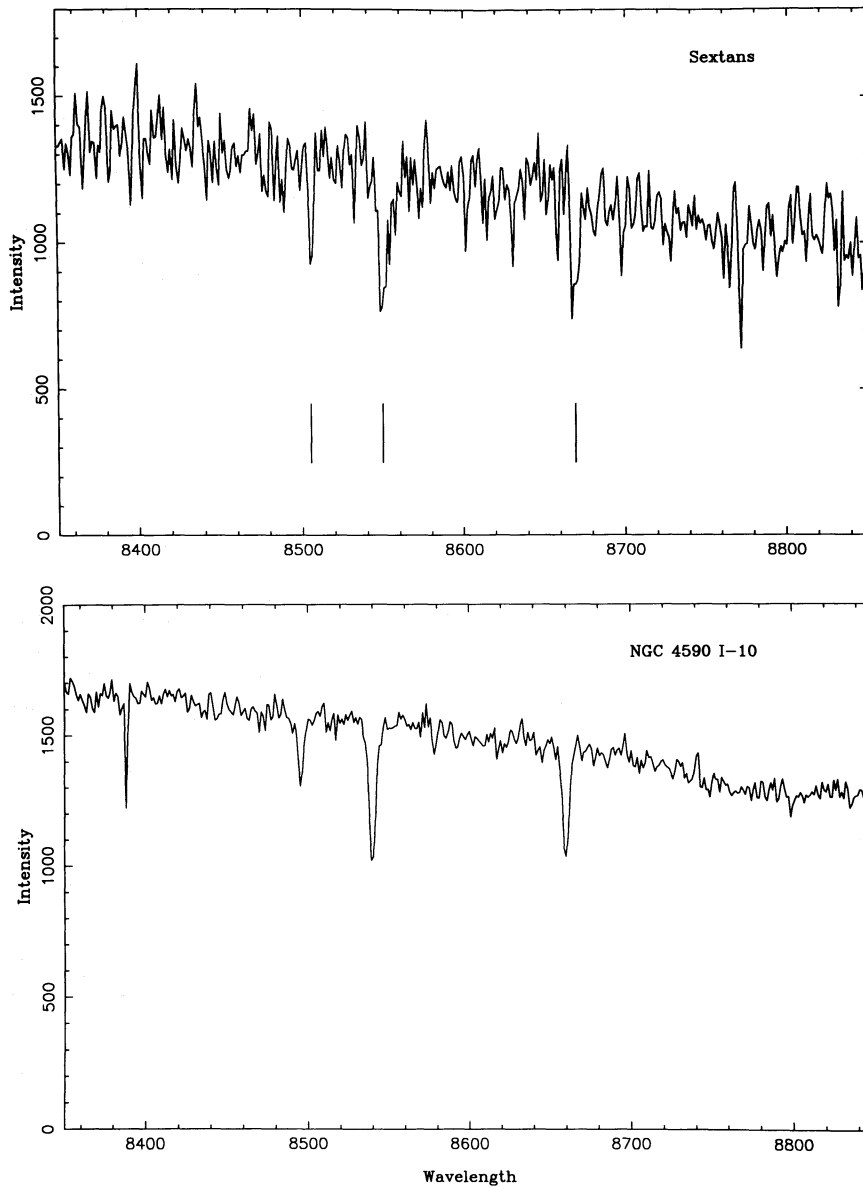
Figure 3. Upper panel: a composite spectrum made by summing the individual spectra of the six Sextans members. The vertical scale is linear in CCD intensity with zero at the bottom of the panel. The three Ca II lines are indicated. Lower panel: the spectrum of the giant I-10 in the metal-poor globular cluster NGC 4590.

The outermost $(R > 50)$ data points are also plotted individually and they consist of the LMC and SMC (treated as a single object), the eight galactic dSph galaxies and the six outer halo globular clusters with well-established velocities and distances. The location of Sextans is indicated by the circled plus sign. The logarithm of the mean value of $3 v_r^2$ for these 15 outer halo objects is also plotted as a filled square in the figure. Also shown on this plot is the line for a circular velocity V_c of 220 km s^{-1} and lines representing constant values of RV_c^2/G equal to 10^{11} and 10^{12} solar masses. The rms circular velocity of a satellite system is related to the galactic rest frame line-of-sight velocities by the equation $\langle V_c^2 \rangle = 3 \langle v_r^2 \rangle$ if the distribution of satellite orbits is assumed to be isotropic (Lynden-Bell & Frenk 1981).

A number of inferences can be drawn from Fig. 5. First, under the assumption of isotropic orbits, it is clear that the halo globular cluster points are consistent with a circular velocity of 220 km s^{-1} out to at least 40 kpc. Secondly, the equivalent rms circular velocity for the 15 outer halo objects is 155 ± 26 km s^{-1} at a mean distance of a little over 100 kpc. Further, this velocity is only slightly lower (143 ± 25 km s^{-1} at $R \sim 90$ kpc) if the two Leo dSph systems, which are almost twice as far away as the next furthest dSph, are excluded.★

Lynden-Bell *et al.* (1983) used their much lower value (106 ± 18 km s^{-1}) for this velocity to argue that the majority of the galaxy's mass lies inside this outer satellite system and that therefore point-mass approximations could be

★ As is obvious from Fig. 5, the Leo I dSph galaxy has a unique combination of velocity and distance and thus it can play a pivotal role in mass determinations if it is bound to the galaxy. Since it may not be bound to the galaxy (*cf.* Zaritsky *et al.* 1989), and since the Leo II system is at a comparable distance, we will discuss results both with and without the Leo systems.
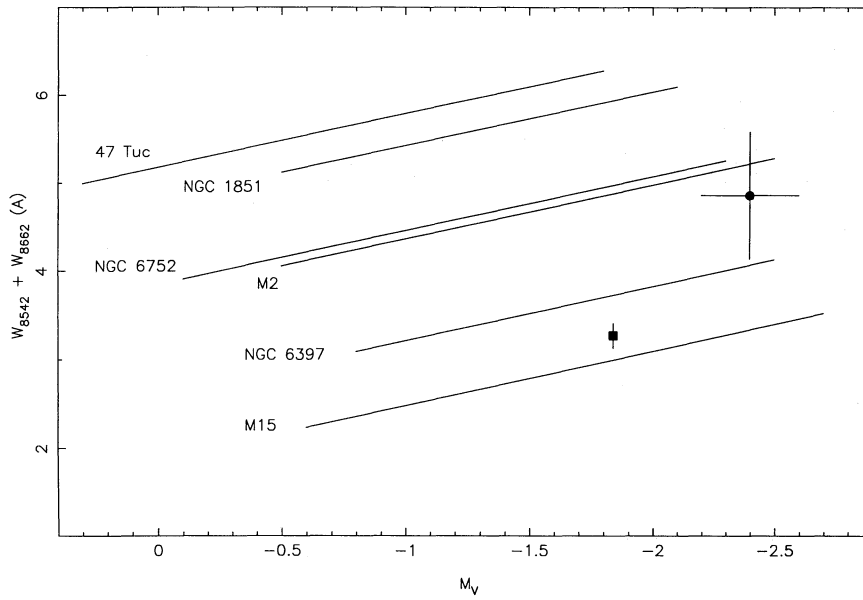
Figure 4. The sum of the equivalent width (in Å) of the Ca II lines at λ8542 and λ8662 is plotted against absolute visual magnitude M_V. The abundances [Fe/H] adopted for the calibrating clusters are: 47 Tuc, −0.71 dex; NGC 1851, −1.29 dex; NGC 6752, −1.54 dex; M2, −1.58 dex; NGC 6397, −1.91 dex; M15, −2.15 dex, respectively. The location of the composite Sextans spectrum is indicated by a filled circle; an uncertainty of ±0.2 mag has been adopted for the M_V value. The NGC 4590 giant location is indicated by a filled square.
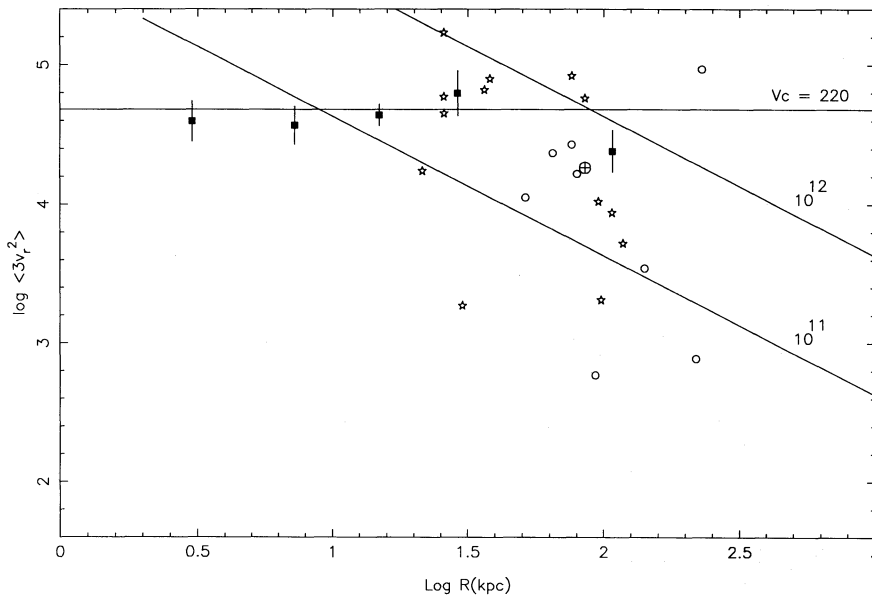
Figure 5. The square of the line-of-sight velocity in the galactic rest frame (v_r) is plotted against galactocentric distance R in kpc for the galaxy's satellites. Filled squares represent averages of $3v_r^2$ in radial bins. The inner four points of this type are the halo globular clusters with the individual clusters shown as star symbols for the $20 < R < 40$ kpc bin. The systems with $R > 50$ kpc are also shown individually; globular clusters by star symbols and galaxies by open circles. Sextans is indicated by the circled plus sign. The outermost filled square is the mean location of these 15 objects. The dSph galaxy with the large values of R and $3v_r^2$ is Leo I. Also shown is a line of constant circular velocity $V_c = 220$ km s^{-1} and lines of constant RV_c^2/G equal to 10^{11} and 10^{12} solar masses.

employed. This is not so obviously the case here, especially as for example, Salucci & Frenk (1989) describe a model for the galaxy with an extended isothermal halo in which the asymptotic (i.e. well outside the optical disc) circular velocity is approximately 180 km s^{-1} while retaining a circular velocity of 220 km s^{-1} in the vicinity of the Sun. Nevertheless, the point-mass approximations (Lynden-Bell *et al.* 1983)

$$M_{\rm gal} = 4\langle Rv_r^2\rangle/G \quad \text{or} \quad M_{\rm gal} = \langle R\rangle\langle V_c^2\rangle/G \quad \text{with} \quad \langle V_c^2\rangle = 3\langle v_r^2\rangle,$$

both of which assume isotropic orbit distributions, yield masses $M_{\rm gal} = 9 \pm 1 \times 10^{11}$ and $6 \pm 2 \times 10^{11}$ $M_\odot$ including the Leo systems, and $M_{\rm gal} = 5 \pm 2 \times 10^{11}$ and $4.5 \pm 1.5 \times 10^{11}$ $M_\odot$ if these systems are excluded. Given that a circular velocity of 220 km s^{-1} at a galactocentric distance of 8.5 kpc implies an interior mass of 1×10^{11} $M_\odot$, it is clear that all these
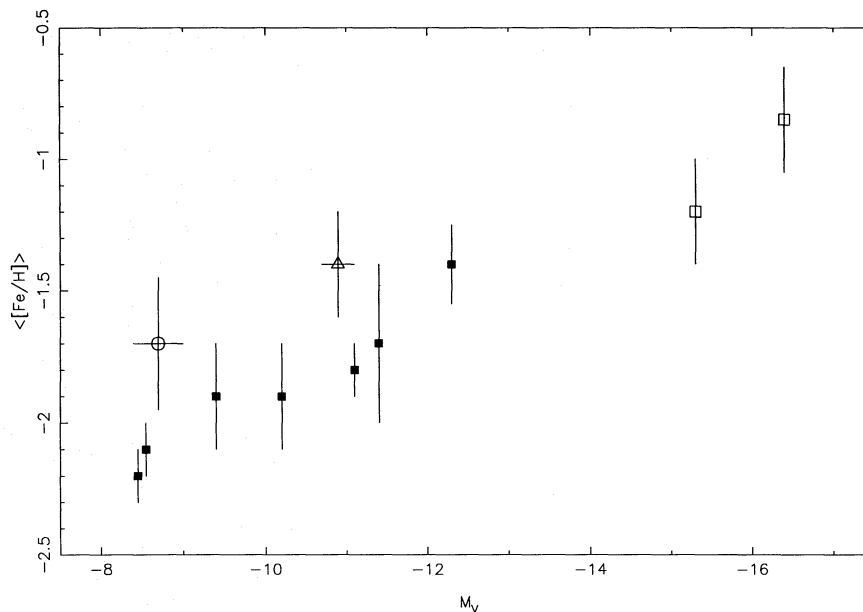
Figure 6. The mean abundance ⟨[Fe/H]⟩ of the galactic and M31 dSph and dE companion galaxies are plotted against their absolute visual magnitudes. Sextans is indicated by the open circle while the open triangle indicates the location of the M31 dSph system And I. The remaining seven galactic dSph galaxies are indicated by filled squares and are, in order of increasing luminosity, Ursa Minor, Draco, Carina, Leo II, Sculptor, Leo I and Fornax. The open squares are, again in order of increasing luminosity, the M31 dE companions NGC 147 and NGC 205.

values indicate the presence of a substantial amount of mass outside the solar circle. We note, however, that there are a number of caveats attached to these numbers. First, the errors given are simply the standard errors of the mean and that the true uncertainties are undoubtedly much larger (*cf.* Zaritsky *et al.* 1989). Secondly, the mass estimates would be reduced if the satellites are on predominantly radial orbits whereas a predominance of tangential orbits would raise the mass estimates. Finally, we note that the circular velocity method, in which v_r^2 and R are averaged separately, is, not surprisingly, less sensitive to whether or not the Leo dSph systems are included in the mass estimate than for the case where the product Rv_r^2 is averaged. These mass determinations are comparable to other recent determinations (Olszewski, Peterson & Aaronson 1986; Little & Tremaine 1987) though they are somewhat lower than those of Zaritsky *et al.* (1990) who place considerable weight on the data for the Leo I system. The difference, however, is within the uncertainties.

We close this section by emphasizing the small size of the outer halo satellite sample with which these analyses are carried out. Given that the distances and velocities are now relatively well known, it is this small sample size that is the largest source of uncertainty. And while the automated search technique that resulted in the discovery of Sextans may yield a further one or two objects (Irwin *et al.* 1990), the galactic dSph galaxies and outer halo globular clusters will never be sufficiently numerous to provide statistically robust results. What is required to tackle this problem are radial-velocity studies of sizeable samples of very distant halo field stars. Such studies are currently underway (Norris & Hawkins 1991).

Turning now to the estimate of the Sextans mean metal abundance derived above, we note that this abundance is

somewhat higher than that expected from the correlation between mean metal abundance and absolute visual magnitude exhibited by the other galactic dSph galaxies (e.g. Da Costa 1988). The data of Da Costa (1988) are reproduced in Fig. 6 with the addition of points for Sextans and for the M31 dSph companion And I (Mould & Kristian 1990). The absolute visual magnitude for Sextans comes from the value $M_B \sim -8$ given by Irwin *et al.* (1990), and the assumption of $(B-V)_0 \sim 0.7$ for an old metal-poor population. This value of M_V is uncertain by at least ± 0.3 mag but it is no less precise than current estimates of the total luminosities of the other dSph galaxies, many of which are quite poorly known.

It is clear from this figure that the Sextans abundance is significantly different, in the sense of being more metal-rich, than those of dSph galaxies of similar luminosities. The M31 dSph also lies off the relation in the same sense. There are at least two explanations for this apparent increase in the scatter in the correlation of Fig. 6.

The first is that the location of Sextans and And I in Fig. 6 reveals for the first time the extent of *intrinsic* scatter in the dSph luminosity–abundance relation. In this context it will be of some interest to see where the other two known M31 dSph companions, And II and And III, fall in this diagram when similar data for them become available. The relation shown in Fig. 6 is usually interpreted as a mass–metallicity relation that is a manifestation of the formation process for dSph galaxies (e.g. Buonanno *et al.* 1985). The presence of intrinsic scatter in such a relation would then argue for a range in formation processes perhaps resulting from, for example, differing relative amounts of dark and 'visible' matter (Dekel & Silk 1986). Alternatively, it may be that the dSph formation process is affected by the properties of, and proximity to, the neighbouring parent galaxy. For example, Silk, Wyse & Shields (1987) have suggested that the distance

from its parent is an important quantity in determining the metal abundance of a dSph galaxy. The fact that Sextans may have a higher abundance than Draco and Ursa Minor is not inconsistent with this latter picture since both these dSph galaxies lie at smaller galactocentric distance than Sextans.

Secondly, with regard to Sextans, it may be that its orbit about the galaxy is such that it has been more strongly affected by the galactic tidal field, resulting in an evolution to its present extremely low density† and low luminosity from an originally more luminous precursor (Kuhn & Miller 1989). Again we must await the difficult measurement of the tangential velocity of this, and other galactic dSph galaxies, before deciding this issue.

NOTE ADDED IN PROOF

In a recent preprint, Mateo *et al.* (1991, *Astr. J.,* in press) have used a colour-magnitude diagram to derive an abundance estimate for Sextans that is similar to the spectroscopic value determined here.

ACKNOWLEDGMENTS

REFERENCES

Aaronson, M. & Olszewski, E. W., 1988. In: *Large-Scale Structures of the Universe, IAU Symp. No. 130,* p. 409, eds Audouze, J., Pelletan, M.-C. & Szalay, A., Kluwer, Dordrecht.
Armandroff, T. E., 1989. *Astr. J.,* **97,** 375.
Armandroff, T. E. & Da Costa, G. S., 1986. *Astr. J.,* **92,** 777.
Armandroff, T. E. & Da Costa, G. S., 1991. *Astr. J.,* **101,** in press.
Buonanno, R., Corsi, C. E., Fusi Pecci, F., Hardy, E. & Zinn, R., 1985. *Astr. Astrophys.,* **152,** 65.
Cannon, R. D., Sagar, R. & Hawkins, M. R. S., 1990. *Mon. Not. R. astr. Soc.,* **243,** 151.
Da Costa, G. S., 1988. In: *Globular Cluster Systems in Galaxies, IAU Symp. No. 126,* p. 217, eds Grindlay, J. & Philip, A. G. D., Kluwer, Dordrecht.
Dekel, A. & Silk, J., 1986. *Astrophys. J.,* **303,** 39.
Delhaye, J., 1965. In: *Stars and Stellar Systems, Vol. 5, Galactic Structure,* p. 61, eds Blaauw, A. & Schmidt, M., University of Chicago, Chicago.
Gilmore, G. & Reid, N., 1983. *Mon. Not. R. astr. Soc.,* **202,** 1025.
Harris, W. E., 1975. *Astrophys. J. Suppl.,* **29,** 397.
Hesser, J. E., Shawl, S. J. & Meyer, J. E., 1986. *Publs astr. Soc. Pacif.,* **98,** 403.
Hodge, P. W., 1964a. *Astr. J.,* **69,** 438.
Hodge, P. W., 1964b. *Astr. J.,* **69,** 853.
Irwin, M. J., Bunclark, P. S., Bridgeland, M. T. & McMahon, R. G., 1990. *Mon. Not. R. astr. Soc.,* **244,** 16P.
Kuhn, J. R. & Miller, R., 1989. *Astrophys. J.,* **341,** L41.
Little, B. & Tremaine, S., 1987. *Astrophys. J.,* **320,** 493.
Lynden-Bell, D., Cannon, R. D. & Godwin, P. J., 1983. *Mon. Not. R. astr. Soc.,* **204,** 87P.
Lynden-Bell, D. & Frenk, C. S., 1981. *Observatory,* **101,** 200.
Olszewski, E. W., Peterson, R. C. & Aaronson, M., 1986. *Astrophys. J.,* **302,** L45.
Mould, J. & Kristian, J., 1990. *Astrophys. J.,* **354,** 438.
Norris, J. & Hawkins, M. R. S., 1991. *Astrophys. J.,* submitted.
Pryor, C. & Kormendy, J., 1990. *Astr. J.,* **100,** 127.
Salucci, P. & Frenk, C. S., 1989. *Mon. Not. R. astr. Soc.,* **237,** 247.
Silk, J., Wyse, R. F. G. & Shields, G. A., 1987. *Astrophys. J.,* **322,** L59.
Zaritsky, D., Olszewski, E. W., Schommer, R. A., Peterson, R. C. & Aaronson, M., 1989. *Astrophys. J.,* **345,** 759.
Zinn, R., 1985. *Astrophys. J.,* **293,** 424.
Zinn, R. & West, M. J., 1984. *Astrophys. J. Suppl.,* **55,** 45.

† The central surface density of Sextans is a factor of 2.5 less than that of Carina (Irwin *et al.* 1990) and a factor of 5 to 6 less than that of Ursa Minor and Draco (Hodge 1964a, b).